International Journal of Thermofluid Science and Technology (2024)
Volume 11, Issue 1, Paper No. 110104
https://doi.org/10.36963/IJTST.2024110104
Research Article

Numerical comparative study of heat transfer enhancement using three kinds of nanofluids

Abdelkrim Bouaffane
Mechanical Engineering Department, Faculty of Sciences and Technology, Echahid Cheikh Larbi Tebessi University, Tebessa - Algeria

ATICLE INFO

Received: 04 Nov. 2023;
Received in revised form:
21 Dec. 2023;
Accepted: 16 Jan. 2024;
Published online:
24 Jan. 2024

Keywords:
Heat transfer enhancement
Nanofluid
Pressure drop
Pumping power
Friction factor

ABSTRACT

This numerical research is done on the hydrodynamic and thermal characteristics of laminar forced convection of different nanofluids inside horizontal tube. The tube wall is subjected to a constant heat flux condition. Al_2O_3-water, Cu-water, and SiO_2-water are the three considered nanofluids examined in this study. The mathematical model of the present problem is based on the single phase approach, the governing equations are solved iteratively using the finite volume method. For nanoparticle volume fractions ϕ ranging from 0 to 6% and for two values of Reynolds numbers Re=1000 and 2000, Nusselt number, pressure losses (or pumping power), average friction factor and Performance evaluation criterion (PEC) are shown and discussed. The results demonstrate that the increase of ϕ enhances significantly the average Nusselt number particularly for Cu-water and Al_2O_3-water. When nanoparticles are added to pure water, the pumping power is negatively impacted because the augmentation of ϕ leads to increase the pressure drop. The highest pressure drop is occurred for Cu-water followed by Al_2O_3-water and SiO_2-water. The comparison between the studied fluids indicates that the PEC values of Cu-water and Al_2O_3-water are greater than the unity, because they show a significant improvement in the rate of heat transfer with acceptable pressure losses. In the other hand, the PEC values related to SiO_2-water are close to the unity due to the slight increase in average Nusselt number. Therefore, SiO_2-water is ineffective for enhancing the convection heat transfer.

1. Introduction

In recent years, researchers have paid great attention to the phenomenon of flow and heat transfer of nanofluids in various geometries and under different conditions. This interest is not only related to theoretical considerations, but is also relevant to many industrial applications where the understanding and the controlling of these complex phenomena for different types of nanofluids is essential to achieve the best and practical results. The applications of nanofluids are extremely important in thermal engineering industries especially in the heat transfer enhancement such as electric cooling, air conditioning, refrigeration and heat exchanger. Addition of nanoparticles to the based fluid is considered as one of the efficient techniques to enhance the convection heat transfer. This technique was used by many researchers [1-9].

*Corresponding e-mail: abdelkrim.bouaffane@univ-tebessa.dz (Abdelkrim Bouaffane)

Nomenclature

Cp	Specific heat capacity, $J.kg^{-1}.K^{-1}$	*z*	Axial coordinate, m
D	Internal diameter of tube, m	*Greek symbols*	
fr	Friction factor	ϕ	Particle volume concentration
h	Convection coefficient, $W.m^{-2}.K^{-1}$	μ	Fluid dynamic viscosity, $kg.m^{-1}.s^{-1}$
L	Tube length, m	ρ	Fluid density, $kg.m^{-3}$
Nu	Nusselt number	λ	Thermal conductivity, $W.m^{-1}.K^{-1}$
P	Pressure, Pa	θ	Dimensionless temperature
P^*	Dimensionless pressure	*Subscripts*	
Pr	Prandtl number	*av*	average value
q_w	Wall heat flux, $W.m^{-2}$	*b*	bulk value
r	Radial coordinate, m	*bf*	Base-fluid
r_0	Inner radius of tube, m	*in*	Inlet
Re	Reynolds number	*nf*	Nanofluid
T	Fluid temperature, K	*out*	Outlet
U	Axial velocity, m. s^{-1}	*p*	Particle
V	Radial velocity, m. s^{-1}	*w*	Wall

The convective heat transfer in nanofluids can be performed using two different models single-phase and two-phase models. In the single phase model (or homogeneous model) is valid for fluids with suspended nanosize particles. This model assumes that the base fluid and nanoparticles are in chemical and thermal equilibrium and the relative velocity between fluid and solid phases is equal to zero. This assumption is reasonable when the nanoparticles are uniformly distributed in base fluids, thus it can be considered as a single fluid. In the two-phase model base fluid and nanoparticles are considered as two different liquid and solid phases with different momentums respectively [10-13].

Many analytical, numerical and experimental investigations have been performed for heat transfer improvement using nanofluids [14]. A review focused in the topic of the improvement of the convection heat transfer using nanofluids. For exemple, Bianco et al. [15] studied numerically laminar forced convection of alumina-water nanofuid in horizontal heated circular tube. Single-phase and two-phase models were employed. The results show that the maximum difference in the average convection coefficient between single and two-phase models results is approximately 11%. They prove also that the heat transfer improves by increasing the particle volume concentration or Reynolds number, but this improvement is accompanied by an increase of shear stress. Maiga et al [16] explored the characteristics of laminar flow of nanofluids inside two distinct geometries: in a straight heated tube and in a radial space between coaxial and heated disks. Two nanofluids were considered, Ethylene Glycol-γAl_2O_3 and water-γAl_2O_3. Results have clearly revealed that the addition of nanoparticles has produced a remarkable increase of the heat transfer with increasing of particle volume concentration.

In an experimental research, Almohammadi et al. [17] investigated the thermal convective heat transfer of nanofluid Al_2O_3-water in laminar flow through a circular tube under the conditions of constant heat flux. In comparison to distilled water, it was found that the average coefficient of heat transfer increased by about 11–20% for a volume concentration ϕ=0.5% and by about 16–27% for ϕ=1%. Furthermore, at ϕ=0.5% volume concentration, the friction factor for nanofluids does not significantly rise. Zeinali et al. [18] measured the convective heat transfer coefficient of laminar flow of Cu-watre nanofluid through inside square duct submitted to a uniform heat flux. Their experimental results revealed that a remarkable increase in heat transfer coefficient is obtained compared to the base fluid. Moreover, it has been achieved that heat transfer coefficient improved

with increasing concentration of nanoparticles in the nanofluid as well as nanofluid flow rate. An increase of 20.7% in Nusselt number achieved at ϕ=1.5%. Benzeggouta et al. [19] numerically investigated laminar convective heat transfer of Al_2O_3-water and Cu-water through horizontal tube under uniform heat flux. They found an increase in heat transfer at several volume fractions for two used nanofluids. They prove also that nanofluids can also contributes to optimize pipes compactness, using 2% alumina and 4% for copper dispersed in water. Laminar forced convection in a circular tube was numerically investigated by Nilesh [20]. Three nanofluids, TiO2-water, Al2O3-water and ZrO2-water are examined under constant heat flux boundary condition. It was shown that the heat transfer coefficient achieved by the employment of nanofluids is significantly higher as compared to the base fluid. The performance factor of nanofluids is found to be poor and the increase of particle loading the decreases the performance factor.

Zeinali et al. [21] studied numerically the effect of CuO-water and Al_2O_3-water nanofluids on the convective heat transfer and pressure losses for the case of in laminar flow inside square and triangular duct. It was observed that heat transfer coefficient of nanofluid increases in comparison with that of pure water. The Nusselt number increases by increasing the concentration and decreasing the nanoparticles size. The results show that the addition of nanoparticles increases the pressure drop in square and triangular ducts. They also found that the pressure drop occurred from CuO-water nanofluid is higher as compared with Al_2O_3-water nanofluid. Madani et al. [22] investigated numerically the effect of spacing between ribs on the flow and heat transfer of Al_2O_3-water nanofluid through a horizontal micro-channel. The volume concentration of nanoparticles ϕ varied from (0-4%). The results showed that the increase of ϕ and Reynolds number significantly ameliorate the Nusselt number. Reynolds number leads to increase the Nusselt and the Poiseuille number. Also, adding ribs in microchannel wall enhances the nusselt number. However, the increase of spacing between ribs leads to reduce the heat transfer. Mostafa et al. [23] performed simulations to investigate the heat transfer coefficient of Al_2O_3-water nanofluid in the developed region of tube flow under constant heat flux. Effect of particle size on convective heat transfer coefficient was studied for (*Re*=500-2500). It was reported that the heat transfer coefficient improved with increasing ϕ and *Re*. The convection coefficient decreased with increasing the particle diameter. Krishna [24] investigated experimentally the effect of ZnO-water nanofluid on the forced convection inside a concentric tube heat exchanger for (Re=2000-5000) and at different ϕ (ϕ=0.1-0.5%). The results indicate that the heat transfer coefficient of ZnO-water nanofluid enhances by increasing ϕ in base fluid. It is also shown for ϕ=0.5%; the overall coefficient of heat transfer is improved by 11% in comparison with pure water. Praveen et al. [25] conducted an experimental study to determine the friction factor and heat transfer coefficient for the flow of a fly ash nanofluid in a copper tube under a boundary condition of constant heat flux. fly ash-water nanofluid is used with ϕ range 0.5–2.0 %. They demonstrate that the increase in Nusselt number (Nu) and friction factor was 46.9% and 9.89%, respectively, at 2.0%.when compared to the base fluid. The maximum PEC value of 1.42 was observed at 2 % for fly ash nanofluid. The maximum PEC value of 1.42 was recorded at 2 vol%. Praveen et al. [26] investigated experimentally and numerically the forced convection heat transfer and flow characteristics of a water base fly ash-Cu (80:20% by volume) hybrid nanofluid (HNF) flow inside a copper tube. The results are presented for concentration of 0.5–2.0 vol%. According to their findings, the highest increases in Nusselt numbers for fly ash nanofluid (FANF) and HNF, respectively, were 8.95% and 57.1% at a concentration of 2.0% relative to water. HNF has a higher pressure drop than FANF and water. They found also that thermal performance factor (TPF) values increase with concentration, the maximum TPF value of 1.52 is recorded at 2% concentration. The addition of nanoparticles to the conventional base fluids has an effect on the variation of friction factor, pressure drop and pumping power of nanofluids flows in ducts. Therefore, many researchers performed several studies to find the influence of different nanofluids on the convective heat transfer; friction factor and pressure drop [27, 36].

The current literature reveals that the addition of nanoparticles to pure fluids represents an efficient technique to the enhancement of convection heat transfer, but

this technique is accompanied by the negative influence of increase in pressure losses which leads to increase the cost of pumping power. For this reason, the present work investigates numerically laminar forced convection of three different nanofluids flowing in a horizontal tube submitted to a constant and uniform heat flux. Also, this study aims to compare between the PEC factors of the studied nanofluids and showing the type of nanoparticles which produces higher heat transfer with reasonable cost of the pumping power.

2. Problem statement

The geometry of the physical problem is illustrated in Fig.1. The analysis is carried out for laminar convection heat transfer of three different types of nanofluids inside horizontal cylindrical tube. The nanofluid enters the tube with uniform velocity U_{in}, uniform temperature T_{in} and absorbs the heat from the wall of the tube which exposed to a uniform heat flux q_w.

The present study is based on the following assumptions:

- Stationary and axisymmetric flow
- Homogeneous and incompressible nanofluid
- Viscous dissipation, thermal radiation and gravitational effects are ignored.
- Base fluid and nanoparticles are in chemical and thermal equilibrium
- Properties of nanofluids are regarded independents to the temperature.

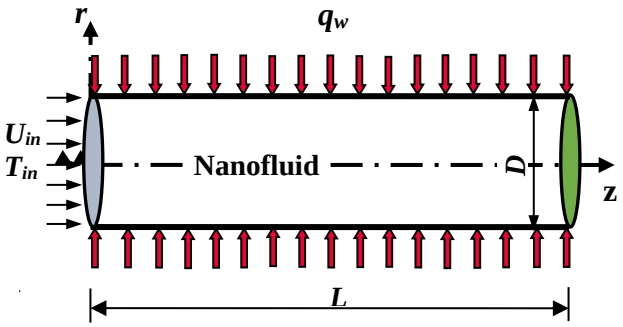

Fig. 1 Schematic of the physical problem

3. Mathematical formulation

3.1 Governing equations

For the case of low concentrations of nanoparticles and small sizes of particles, the nanofluids are assumed to be homogeneous and considered as single phase fluids [37]. In this paper, the single-phase approach is employed to model the laminar forced convection of nanofluid inside circular tube. After introducing the assumptions and conditions of this study to the mathematical model presented in [15,30,38,45,46], the continuity, momentum and energy equations can be written as follow:

- Continuity equation:

$$\frac{1}{r}\frac{\partial(rV)}{\partial r}+\frac{\partial U}{\partial Z}=0 \tag{1}$$

- Momentum equation in radial direction:

$$\rho_{nf}\left(V\frac{\partial V}{\partial r}+U\frac{\partial V}{\partial Z}\right)=-\frac{\partial P}{\partial r}+\mu_{nf}\left[\frac{1}{r}\frac{\partial}{\partial r}\left(r\frac{\partial V}{\partial r}\right)-\frac{V}{r^2}+\frac{\partial^2 V}{\partial Z^2}\right] \tag{2}$$

- Momentum equation axial direction:

$$\rho_{nf}\left(V\frac{\partial U}{\partial r}+U\frac{\partial U}{\partial Z}\right)=-\frac{\partial P}{\partial Z}+\mu_{nf}\left[\frac{1}{r}\frac{\partial}{\partial r}\left(r\frac{\partial U}{\partial r}\right)+\frac{\partial^2 U}{\partial Z^2}\right] \tag{3}$$

- Energy equation:

$$(\rho Cp)_{nf}\left(V\frac{\partial T}{\partial r}+U\frac{\partial T}{\partial Z}\right)=\lambda_{nf}\left[\frac{1}{r}\frac{\partial}{\partial r}\left(r\frac{\partial T}{\partial r}\right)+\frac{\partial^2 T}{\partial Z^2}\right] \tag{4}$$

3.2 Nanofluids thermophysical properties

- The effective density of the nanofluid is presented in [39] as:

$$\rho_{nf}=(1-\emptyset)\rho_{bf}+\emptyset\rho_p \tag{5}$$

- The dynamic viscosity of nanofluid is given by Brinkman [40] as:

$$\mu_{nf}=\mu_{bf}(1-\emptyset)^{-2.5} \tag{6}$$

- The heat capacity of the nanofluid is expressed in [11,33,41,53] as:

$$\left(\rho C_p\right)_{nf}=(1-\emptyset)\left(\rho C_p\right)_f+\emptyset\left(\rho C_p\right)_p \tag{7}$$

- The thermal conductivity of nanofluids can be calculated from Maxwell model [41,42]:

$$\lambda_{nf}=\lambda_{bf}\left[\frac{\lambda_p+2\lambda_{bf}-2\emptyset(\lambda_{bf}-\lambda_p)}{\lambda_p+2\lambda_{bf}+\emptyset(\lambda_{bf}-\lambda_p)}\right] \tag{8}$$

In the above equations ϕ represent the volume fraction of nanoparticles and named also volume concentration of nanoparticles, is defined in [2] as the ratio of nanoparticles volume (V_p) to the total volume (V_T):

$$\emptyset=\frac{V_P}{V_T} \tag{9}$$

3.3 Boundary conditions

The Dynamic and thermal boundary conditions of the studied phenomenon are presented in Table 1

Table 1 Dynamic and thermal conditions

Limit	Dynamic and thermal conditions
Inlet	$U = U_{in}\ , V = 0, T = T_0$
outlet	$\frac{\partial U}{\partial z} = \frac{\partial V}{\partial z} = \frac{\partial T}{\partial z} = 0$
Centerline	$\frac{\partial U}{\partial r} = \frac{\partial V}{\partial r} = \frac{\partial T}{\partial r} = 0$
Wall	$U = V = 0, \quad \lambda_{nf}\frac{\partial T}{\partial r} = q_w$

3.4 Dimensionless governing equations

In order to identify the dimensionless parameters that govern this phenomenon, it is necessary transforming the dimensional form of the model to the dimensionless form by introducing the following dimensionless variables (Z^*, r^*, U^*, V^*, θ, P^*) in equations (1) to (4) and boundary conditions [43]:

$$Z^* = \frac{Z}{D}\ ,\ r^* = \frac{r}{D}\ ,\ U^* = \frac{U}{U_{\text{in}}},\ V^* = \frac{V}{U_{\text{in}}},$$
$$P^* = \frac{P}{\rho_{nf}U_{\text{in}}^2}\ ,\ \theta = \left(\frac{\lambda_{nf}}{\dot{q}_w D}\right)(T - T_{\text{in}})$$

The set of equations (1-4) and boundary conditions becomes as follow:

- Continuity equation:

$$\frac{1}{r^*}\frac{\partial(r^*V^*)}{\partial r^*} + \frac{\partial U^*}{\partial Z^*} = 0 \qquad (10)$$

- Momentum equation in axial direction:

$$\frac{1}{r^*}\frac{\partial(r^*V^*U^*)}{\partial r^*} + \frac{\partial(U^*U^*)}{\partial Z^*} = -\frac{\partial P^*}{\partial Z^*} + \frac{1}{Re_{nf}}\left[\frac{1}{r^*}\frac{\partial}{\partial r^*}\left(r^*\frac{\partial U^*}{\partial r^*}\right) + \frac{\partial}{\partial Z^*}\left(\frac{\partial U^*}{\partial Z^*}\right)\right] \qquad (11)$$

- Momentum equation in radial direction:

$$\frac{1}{r^*}\frac{\partial(r^*V^*V^*)}{\partial r^*} + \frac{\partial(U^*V^*)}{\partial Z^*} = -\frac{\partial P^*}{\partial r^*} + \frac{1}{Re_{nf}}\left[\frac{1}{r^*}\frac{\partial}{\partial r^*}\left(r^*\frac{\partial V^*}{\partial r^*}\right) - \frac{V^*}{r^{*2}} + \frac{\partial}{\partial Z^*}\left(\frac{\partial V^*}{\partial Z^*}\right)\right] \qquad (12)$$

- Energy equation:

$$\frac{1}{r^*}\frac{\partial(r^*V^*\theta)}{\partial r^*} + \frac{\partial(U^*\theta)}{\partial Z^*} = \frac{1}{Re_{nf}.Pr_{nf}}\left[\frac{1}{r^*}\frac{\partial}{\partial r^*}\left(r^*\frac{\partial\theta}{\partial r^*}\right) + \frac{\partial}{\partial Z^*}\left(\frac{\partial\theta}{\partial Z^*}\right)\right] \qquad (13)$$

Where:

$$Re_{nf} = \frac{\rho_{nf}U_{in}D}{\mu_{nf}} \qquad (14)$$

$$Pr_{nf} = \frac{\mu_{nf}\ C_{p_{nf}}}{\lambda_{nf}} \qquad (15)$$

From equations (10) to (13), it can be seen that the problem under study is related to Reynolds number (Re_{nf}), Prandtl number (Pr_{nf}) and the particle concentration ϕ. It should be noted that Reynolds and Prandtl numbers of based fluid are written as follow:

$$Re_{bf} = Re_{nf}(\emptyset = 0) = \frac{\rho_{bf}U_{in}D}{\mu_{bf}} \qquad (16)$$

$$Pr_{bf} = Pr_{nf}(\emptyset = 0) = \frac{\mu_{bf}\ C_{p_{bf}}}{\lambda_{bf}} \qquad (17)$$

3.5 Dimensionless boundary conditions

The boundary conditions in dimensionless form are presented in Table 2:

Table 2 Dimensionless boundary conditions

Limit	Dynamic and thermal conditions
Inlet	$U^* = 1,\ V^* = 0\ ,\ \theta = 0$
Outlet	$\frac{\partial U^*}{\partial z^*} = \frac{\partial\ V^*}{\partial z^*} = \frac{\partial\theta}{\partial z^*} = 0$
Centerline	$\frac{\partial U^*}{\partial r^*} = \frac{\partial\ V^*}{\partial r^*} = \frac{\partial\theta}{\partial r^*} = 0$
Wall	$U^* = V^* = 0\ ,\ \frac{\partial\theta}{\partial r^*} = 1$

4. Determination of the hydrodynamic and thermal parameters

4.1 Nusselt Number

The local convection heat transfer coefficient h(z*)* is defined as follow [47]:

$$q_w = h(z)[T_w(z) - T_b(z)] \qquad (18)$$

Here, $T_w(z)$ and $T_b(z)$ are respectively the temperature of the wall and the bulk temperature of fluid at the cross section z. The local Nusselt number *Nu(z)* is obtained by writing equation (18) in dimensionless form:

$$Nu(z) = \frac{h(z)D}{\lambda_{bf}} = \frac{\lambda_{nf}}{\lambda_{bf}}\left[\frac{1}{\theta_w(z) - \theta_b(z)}\right] \qquad (19)$$

$\theta_w(z)$ and $\theta_b(z)$ are respectively the dimensionless temperature of the wall and the dimensionless bulk temperature of fluid. The rate of heat transfer is evaluated by calculating the average convection coefficient 'h_{av}' or the average Nusselt number 'Nu_{av}' which are expressed as:

$$h_{av} = \frac{1}{L}\int_0^L h(z)\,dz \qquad (20)$$

$$Nu_{av} = \frac{h_{av}D}{\lambda_{bf}} = \frac{1}{(L/D)}\int_0^{L/D} Nu(z^*)\,dz^* \qquad (21)$$

4.2 Friction factor

The expression of local friction factor presented in [48] can be written for the case of nanofluid flow inside tubes as follow:

$$fr(z) = -\frac{2D}{\rho_{nf}U_{in}^2}\frac{dP}{dZ} \qquad (22)$$

The average friction factor fr_{av} is expressed as:

$$fr_{av} = \frac{1}{L}\int_0^L fr(Z)\,dZ \qquad (23)$$

4.3 Pressure drop and pumping power

Pressure losses inside tube and required pumping power are defined respectively as:

$$\Delta P = P_{in} - P_{out} \qquad (24)$$

$$PP = U_{in}(\pi D^2/4)\Delta P \qquad (25)$$

4.4 Performance evaluation criterion

Performance evaluation criterion (PEC) is also named 'thermal-hydraulic performance' or 'overall thermal performance factor'. For a judicious choice of operating conditions that ensures a considerable enhancement in the heat transfer without a large increase in the pumping power, the parameter PEC constitutes an important factor in the construction of heat exchangers. The heat transfer enhancement technology can be considered useful and efficient only if (PEC>1). The thermal performance PEC is defined in [32,34,44] as :

$$PEC = \frac{Nu_{av,nf}/Nu_{av,bf}}{\left[fr_{av,nf}/fr_{av,bf}\right]^{1/3}} \qquad (26)$$

Where $Nu_{av,nf}$ and $Nu_{av,bf}$ are the Nusselt numbers of nanofluid and pure water respectively. $fr_{av,nf}$ and $fr_{av,bf}$ are the friction factors of nanofluid and pure water respectively.

5. Procedure of solution and convergence

The finite volume technique is employed for the discretization of the mathematical model by transforming the partial differential equations (continuity, momentum and energy) to a set of algebraic equations. Theses equations are solved iteratively using algorithm SIMPLE (Semi-Implicit Method for Pressure-Linked Equations) of Patankar [49]. The iterative calculations are ensured by a FORTRAN code based on the algorithm TDMA (Tri Diagonal Matrix Algorithm) [50]. The solution is obtained when the computed variables Φ (Φ =*U, V, P, θ*) become invariant with iterations (or negligible variation with iterations). The convergence is controlled by calculating the residual of the algebraic equations obtained from the discretization of the governing equations, the final form of the discretized equations is:

$$A_{i,j}\Phi_{i,j} = A_{i-1,j}\Phi_{i-1,j} + A_{i+1,j}\Phi_{i+1,j} + A_{i,j-1}\Phi_{i,j-1} + A_{i,j+1}\Phi_{i,j+1} + b_{i,j} \qquad (27)$$

The residual $R_{\Phi i,j}$ is calculated at each iteration from equation (27) as follow:

$$R_{\Phi_{i,j}} = A_{i,j}\Phi_{i,j} - A_{i-1,j}\Phi_{i-1,j} - A_{i+1,j}\Phi_{i+1,j} - A_{i,j-1}\Phi_{i,j-1} - A_{i,j+1}\Phi_{i,j+1} - b_{i,j} \qquad (28)$$

The convergence was considered to have been achieved only if the maximum residual in all control volumes of the computational domain is less than 10^{-6}. Figures 2 and 3 illustrate the variation of the average convection coefficient and pressure drop with iterations, it is shown that the solution is approximately converged after 2300 iteration.

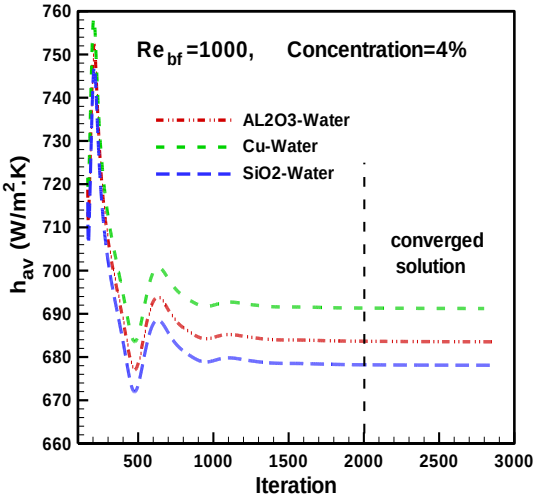

Fig. 2 Variation of h_{av} with iteration

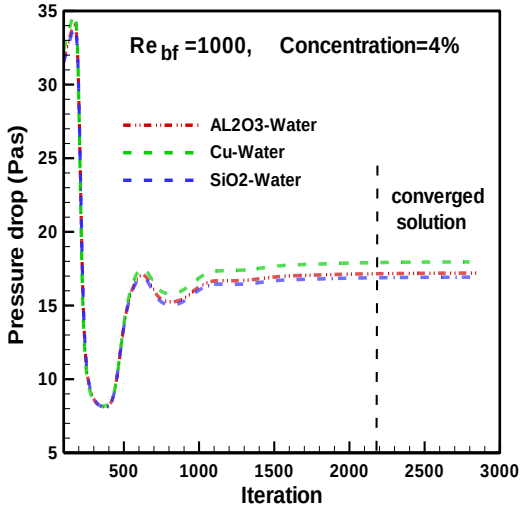

Fig. 3 Variation of pressure drop with iterations

6. Choice of grid

The choice of the mesh of the computational domain is a crucial step in the numerical simulation and has a great influence on the accuracy of the results and the computation time. In order to optimize these parameters, we have performed several simulations on the variation of h_{av} and fr_{av} with different mesh sizes. The results of the simulations are presented in Table 3 at Re_{bf} =1000 and ϕ = 4%. The results show that the mesh size (221x41) is sufficient to ensure high accuracy in the resolution of the studied phenomenon. This choice is based on the stabilization of h_{av} and fr_{av} values, especially for the last three mesh sizes. Any increase in the dimensions of the mesh more than (221x41) increases the execution time without any improvement in the accuracy of the solution.

Table 3 Values of h_{av} and fr_{av} of Al_2O_3-water at Re_{bf}=1000 and ϕ = 4%

Mesh	h_{av}	fr_{av}
11×161	689.76	0.0862
21×181	685.18	0.0866
31×201	684.36	0.0866
41×221	684.32	0.0867
51×241	684.44	0.0867
61×261	684.60	0.0868

7. Validation

In order to verify the accuracy of the present method of solution and the code of calculation, hydrodynamic and thermal comparisons with previous results are performed and presented in Tables 4-6.

7.1 Thermal validation

Tables 4 and 5, show a comparison between the values of h_{av} calculated numerically by the present code and the solution of Bianco [15] for the case of laminar flow of nanofluid inside tube at volume fractions 1% and 4% for Re=250, 500, 750 and 1050. The comparison illustrates a good agreement was found between the results of the present code and those displayed in [15] where the maximum difference as relative error between the two solutions is approximately 3.18%.

Table 4 Comparison between the results of the present code and those of Bianco [15] at ϕ=1%

ϕ=0.01		
Re	h_{av} of present code	Relative error with [15]
250	356	3.01 %
500	426	3.18 %
750	484	2.22 %
1050	542	2.34 %

Table 5 Comparison between the results of the present code and those of Bianco [15] at ϕ=4%

ϕ=0.04		
Re	h_{av} of present code	Relative error with [15]
250	402.22	3.07 %
500	491.5	2.28 %
750	559.8	2.78 %
1050	628.4	1.81 %

7.2 Hydrodynamic validation

The friction factor of laminar developed flow of pure fluid inside cylindrical tube is presented in [51] as follow:

$$fr = \frac{64}{Re_{bf}} \qquad (29)$$

For the case of laminar developed flow of nanofluid inside cylindrical tube the relation (29) can be formulated as:

$$fr = \frac{64}{Re_{nf}} \quad (30)$$

Table 6, shows the comparison between the values of friction factor obtained from the code of the present study and those calculated from Eq. (30). The comparison was done for three kinds of nanoparticles (Al_2O_3, Cu, SiO_2) at ϕ=6% and Re_{bf} =1000. Excellent agreement is confirmed between the present numerical results and those obtained from Eq. (30), where the maximum relative difference is around of 0.26%.

From the two performed comparisons, it is shown that the current method of solution and the present code of calculation are valid for simulating the laminar forced convection phenomenon of various nanofluids inside circular tube at different volumetric concentrations and different conditions.

Table 6 Comparison between fr values of correlation (30) and those of present code

Nanofluid	Re_{bf}	Re_{nf}	fr Eq. (30)	fr (present code)	Relative error (%)
Al_2O_3-water	1000	1009.95	6.337×10^{-2}	6.336×10^{-2}	0.016
Cu-water	1000	1265.82	5.056×10^{-2}	5.069×10^{-2}	0.26
SiO_2-water	1000	919.73	6.958×10^{-2}	6.955×10^{-2}	0.043

8. Results and discussion

The results include the influence of the employment of nanofluids on the average heat transfer and pressure losses for various nanoparticles volume concentrations with two values of Reynolds number Re_{bf} =1000 and 2000. Prandtl number Pr_{bf}=5.887. The dimensionless length of tube (L/D) is fixed at 50. Also, the comparisons between the PEC of different nanofluids will be examined for choosing the nanofluid-type which gives higher improvement in heat transfer with reasonable values of pumping power.

Table 7 Thermophysical properties of water and solids at temperature T_0=300K [52]

Materials	water	Cu	Al_2O_3	SiO_2
ρ[kg/m^3]	997	8933	3970	2220
Cp[J/kg.K]	4177	385	765	745
λ[W/m.K]	0.608	401	36	1.38
μ[kg/m.s]	857×10^{-6}	-	-	-

8.1 Effect of nanoparticles concentration on the convection coefficient

The effect of nanoparticles concentration of Al_2O_3, Cu and SiO_2 on the average convection coefficient is presented in Fig.4 (a-b) at Re_{bf} =1000 and 2000 for ϕ varied from 0 to 6%. Heat flux value is fixed at q_w=10000 W/m^2, D=10^{-2}m. The obtained results revealed that:

- The addition of nanoparticles to the pure water has a positive effect on h_{av}, where the values of h_{av} of nanofluids are greater than those of base fluide (pure water)
- The increase of ϕ improves h_{av} for all types of nanofluids, this is due to the fact that the increase of ϕ increases the thermal conductivity of nanofluid as shown in Fig. 5.
- The considerable enhancement of convection heat transfer using nanofluids is obtained by the nanoparticles Cu and Al_2O_3 , this due to their higher thermal conductivities
- The improvement of h_{av} using SiO_2 is not significant, this due to the low increase in its thermal conductivity
- The values of h_{av} resulted for (Re_{bf} =2000) are greater than those of (Re_{bf} =1000). Therefore, the heat transfer enhancement can be achieved by increasing the flow velocity.
- The maximum enhancement in h_{av} resulted from the addition of nanoparticles is obtained at ϕ=6%. The percentages of enhancement in h_{av} are illustrated in Table 8 at ϕ=6%.

Table 8 Percentages of enhancement in h_{av} at ϕ=6%

Nanoparticles	Cu	Al_2O_3	SiO_2
Re_{bf}=1000	13.93%	11.57%	1.99%
Re_{bf}=2000	14.15%	11.34%	1.74%

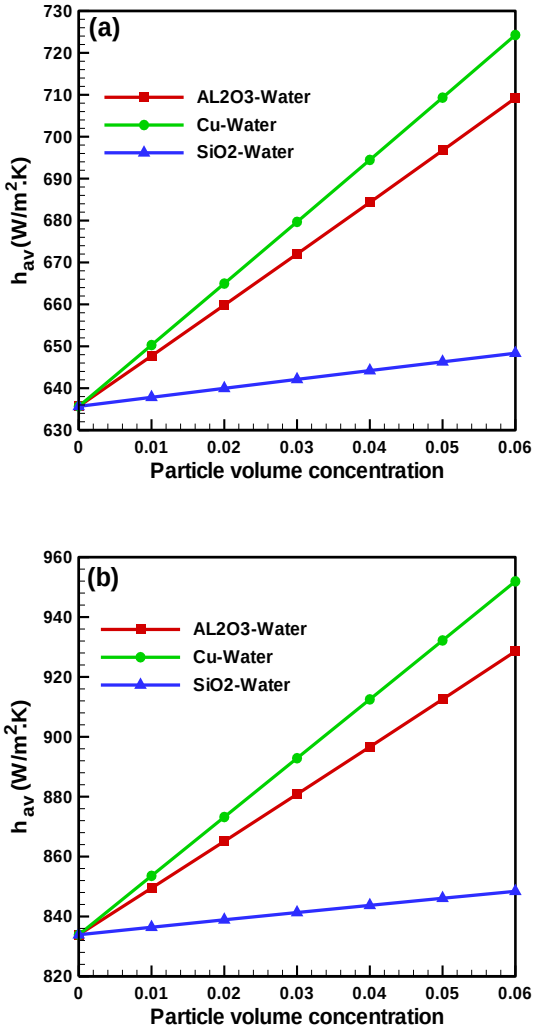

Fig. 4 h_{av} as function ϕ for:
(a) Re_{bf} =1000; (b) Re_{bf} =2000

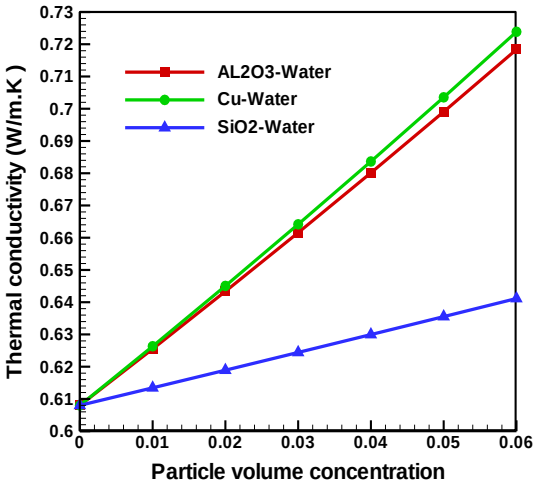

Fig. 5 Nanofluid thermal conductivity versus ϕ

8.2 Effect of nanoparticles concentration on the pressure drop

The previous section the results shows that the employment of nanofluid has a positive effect on the heat transfer, but it is important to know its influence on the pressure drop.

In this section, the variation of pressure drop inside tube versus volumetric concentration ϕ is displayed in Fig. 6 (a-b), where ϕ is varied from 0 to 6%. It can be seen that:

- The pressure drop is proportional to the concentration, where all types of nanofluids studied in this work have a negative effect on the pressure drop if compared with base fluid (pure water), because the augmentation of ϕ produces a clear increase in the pressure losses. Consequently, increases the pumping power
- Any increase in the volumetric concentration increases the density of nanofluid as illustrated in Fig. 7. The increase in density is the main reason for more pressure losses.
- Nanofluid Cu-water offers the highest pressure drop because it has higher density. The medium and the lowest pressure drop are occurred for Al_2O_3-water and SiO_2-water respectively
- For all nanofluids tested in this simulation, the pressure drop calculated for (Re_{bf} =2000) are greater than that of (Re_{bf} =1000). Therefore, the pumping power increases by increasing the velocity of flow.
- The highest increase in pressure losses caused by the presence of different nanoparticles in pure water is found at volumetric concentration ϕ=6%. The percentages of increase in pressure drop are presented in Table 9.

Table 9 Percentages of increase in pressure drop at ϕ=6%

Nanoparticles	Cu	Al_2O_3	SiO_2
Re_{bf} =1000	24.3%	17%	14.3%
Re_{bf} =2000	26.7%	17.1%	13.5%

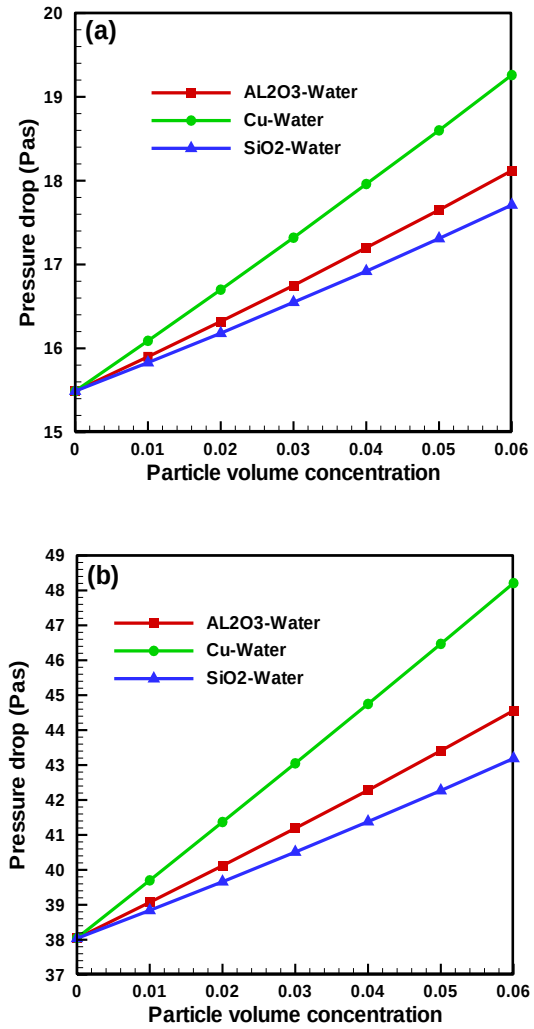

Fig. 6 Pressure drop as function of ϕ for: (a) Re_{bf} =1000; (b) Re_{bf} =2000

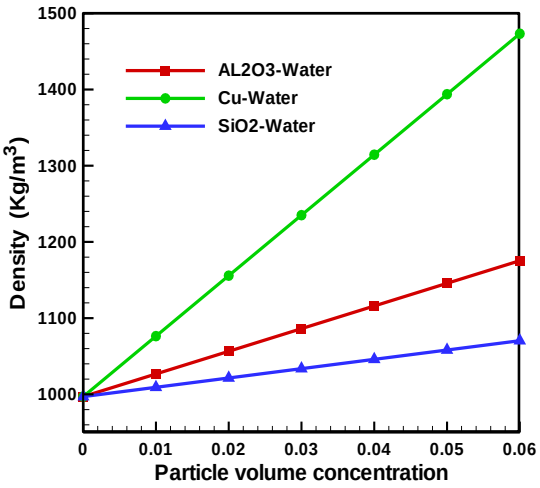

Fig. 7 Nanofluid density versus ϕ

8.3 Effect of nanoparticles concentration on the friction factor

As known the friction factor is dependent to the flow regime (i.e. value of Reynolds number). Then, for analyzing the influence of nanoparticles addition on the average friction factor, it is necessary to calculate the Reynolds number of each nanofluid at different concentration. Fig.8 (a-b) demonstrates that the Reynolds number is affected by the type and the concentration of nanoparticles. Also, Equation (30) shows that the friction factor in the fully developed laminar flow is inversely proportional to Reynolds number. The influence of concentration on the fr_{av} is presented in Fig. 9 (a-b). It appears clearly that:

- The values of friction factor obtained from the present simulation show a good agreement with Eq. (30).
- For Cu-water, the Reynolds number increases by increasing ϕ, consequently the friction factor decreases
- For SiO_2-water, Reynolds number decreases by increasing ϕ, this leads to increase the friction factor.
- For Al_2O_3-water, the friction factor is slightly decreases by increasing ϕ because the Reynolds number increases with very small values.

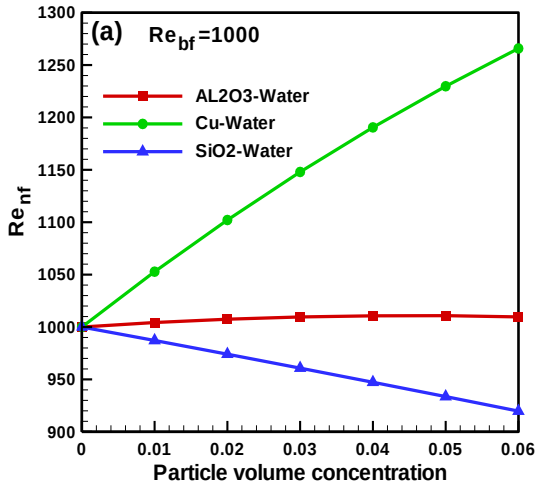

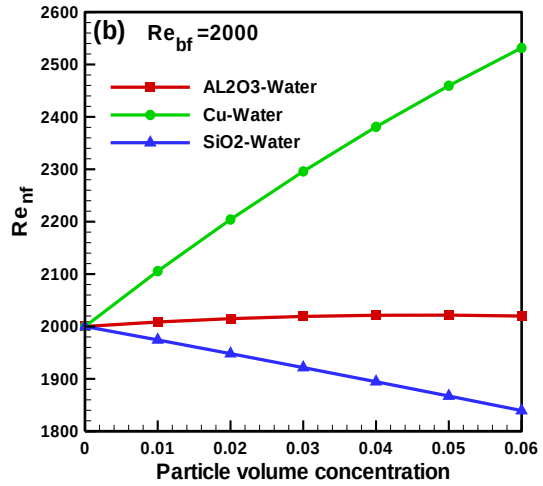

Fig. 8 Nanofluid Reynolds number versus ϕ for: (a) Re_{bf} =1000; (b) Re_{bf} =2000

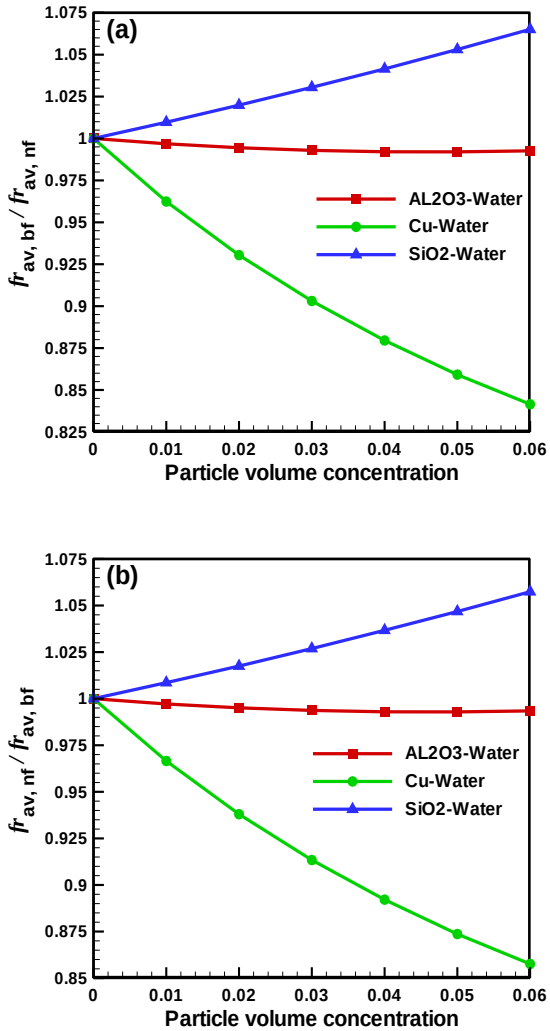

Fig .9 fr_{av} ratio as function of ϕ for: (a) Re_{bf} =1000; (b) Re_{bf} =2000

8.4 Effect of nanoparticles concentration on the PEC factor

The improvement of heat transfer is usually accompanied with the disadvantages of augmentation in pressure losses. For this reason it is required to calculate PEC which shows us the best case to achieve a considerable enhancement in heat transfer with reasonable pumping power. From the correlation of PEC displayed in Eq. (26), it is clear that the PEC factor is dependent to the Nusselt number ratio ($Nu_{av,nf}$ /$Nu_{av,bf}$) and friction factor ratio ($fr_{av,nf}$ /$fr_{av,bf}$). Then, the study of the effect of ϕ on the PEC factor requires displaying the variation of ($Nu_{av,nf}$ /$Nu_{av,bf}$) and ($fr_{av,nf}$ /$fr_{av,bf}$) versus concentration.

Fig. 10 (a-b) shows that the presence of nanoparticles in the pure water has a beneficial influence on the Nusselt number of all nanofluids. The best improvement in Nu_{av} is achieved by Cu-water followed by Al_2O_3-water and SiO_2-water. Because of its greater thermal conductivity, Cu-water provides the highest Nu_{av} enhancement. Also, the variation of friction factor versus ϕ is previously illustrated in Fig. 9 which clearly showed that the increase of nanoparticles concentration leads to increase the friction factor of SiO_2-water (negative effect), decreases friction factor of Cu-water (positive effect) and show a very small decrease in friction factor of Al_2O_3-water (negligible effect). Fig. 11 (a-b) depicts the variation of PEC versus concentration for different nanofluids at Re_{bf} =1000 and 2000. The curves show that:

- All types of nanofluid studied in this research are efficient because theirs PEC is greater than the unity, therefore the improvement of heat transfer using nanoparticles is generally useful
- The SiO_2-water offers the lowest PEC this due to its lower Nu_{av} and higher fr_{av}. In addition, the PEC of SiO_2 is not influenced by the variation of concentration, where its values are approximately equals 1.
- Al_2O_3-water performs a considerable amelioration in the Nu_{av} and stability in fr_{av} with varying ϕ; in this case the values of PEC are greater than the unity.
- The nanofluid Cu-water provides the highest value of Nu_{av} and the lowest value of fr_{av}, theses two features lead to achieve the

maximum values of PEC if compared with Al_2O_3-waters and SiO_2-water.

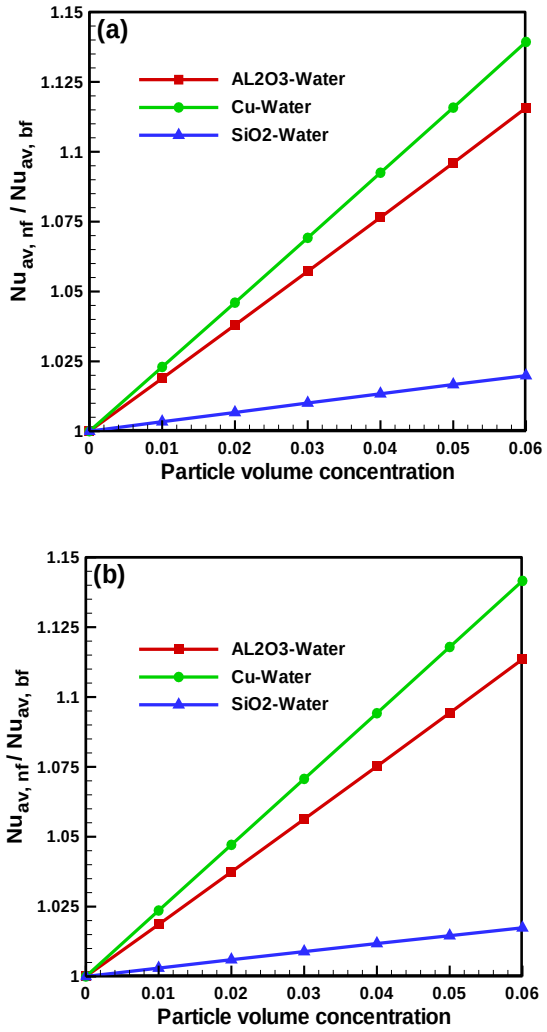

Fig. 10 Variation of Nu_{av} ratio with ϕ for: (a) Re_{bf} =1000; (b) Re_{bf} =2000

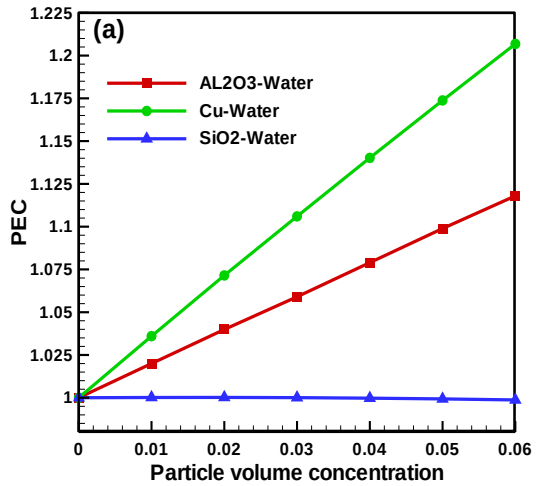

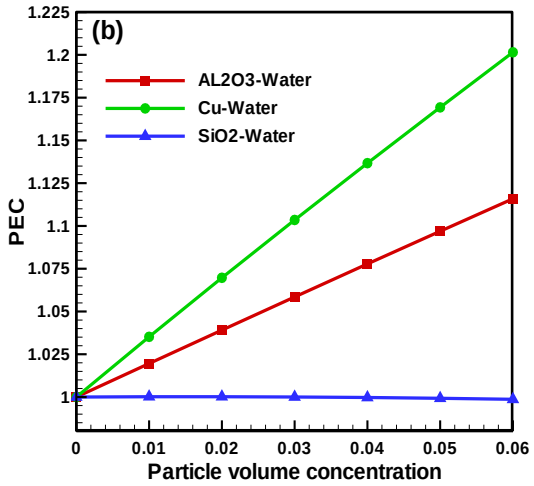

Fig.11 PEC as function of ϕ for: (a) Re_{bf} =1000; (b) Re_{bf} =2000

9. Conclusion

In this paper, hydrodynamic and thermal analysis of laminar flow of three kinds of nanofluids inside cylindrical tube subjected to constant heat flux are investigated numerically. The working base fluid used is pure water. The volume fraction of nanoparticles varied between 0 and 6%. In the range of the operating parameters used in this simulation and from the obtained results, the main conclusions of this study are presented as follow:

- All types of nanofluids show an enhancement in heat transfer if compared with pure water
- Nanoparticles that have high thermal conductivities such as Cu and Al_2O_3 offer a considerable enhancement of convection heat transfer. Where, the best amelioration of Nu_{av} or h_{av} is performed by the nanofluid Cu-water followed by Al_2O_3-water and SiO_2-water.
- The convection coefficient of all types of nanofluids is enhanced by increasing ϕ; this is due to the fact that the increase of ϕ increases the thermal conductivity of nanofluids.
- The addition of nanoparticles has showed a clear negative impact on the pressure drop, because the augmentation of ϕ increases the pressure drop of nanofluids if compared with pure water.
- Any increase in the value of ϕ increases the nanofluid density which leads to elevate the pressure drop as well as increases the pumping power
- The highest pressure drop is occurred with using Cu nanoparticles; this is due to its

higher density. The medium and the lowest values of pressure drop are found for Al_2O and SiO_2 respectively

- The PEC values of both nanofluid Cu-water and Al_2O_3-water are greater the unity, these two nanofluids show a considerable enhancement of heat transfer with acceptable increment in pressure drop. For SiO_2-water all values are approximately equals 1, because it has lower improvement in Nusselt number
- Any increase in ϕ performs to increase the PEC of Cu-water and Al_2O_3-water while SiO_2-water was not influenced by the variation of ϕ.
- Finally, the PEC values indicated that the nanoparticles Cu offers an important improvement of heat transfer with reasonable cost of pumping power in comparison with others studied nanoparticles.

References

[1] M. Elahmer, S. Abboudi, N. Boukadida, Nanofluid effect on forced convective heat transfer inside a heated horizontal tube, International Journal of Heat Technology. 35(2017) 874-882.

[2] A.H. Dhiaa, M.A. Salih, H.A. Al-Yousefi, Effect of ZnO nanoparticles on the thermo-physical properties and heat transfer of nano-fluid flows, International Journal of Heat Technology. 38(2020) 715-721.

[3] C.J. Ho, C.Y. Cheng, T.F. Yang, S. Rashidi, W.M. Yan, Cooling characteristics and entropy production of nanofluid flowing through tube, Alex. Eng. J. 61(2022) 427-441.

[4] A.M. Hussein, H.K. Dawood, R.A. Bakara, K. Kadirgamaa, Numerical study on turbulent forced convective heat transfer using nanofluids TiO_2 in an automotive cooling system, Case Stud. Therm. Eng. 9(2017) 72-78.

[5] Z. Alhajaj, A.M. Bayomy, M.Z. Saghir, M.M. Rahman, Flow of nanofluid and hybrid fluid in porous channels: Experimental and numerical approach, International Journal of Thermofluids.1-2(2020) 100016.

[6] J. Bowersa, H. Caob, G. Qiaoc, Q. Lib, G. Zhangb, E. Murac, Y. Dingb, Flow and heat transfer behavior of nanofluids in microchannels, Progress in Natural Science: Materials International. 28(2018) 225-234.

[7] A. Jafarimoghaddam, S. Aberoumand, An empirical investigation on Cu/Ethylene Glycol nanofluid through a concentric annular tube and proposing a correlation for predicting Nusselt number, Alex. Eng. J. 55(2016) 1047-1052.

[8] H.K. Dawood, H.A. Mohammed, K.M. Munisamy, Heat transfer augmentation using nanofluids in an elliptic annulus with constant heat flux boundary condition, Case Stud. Therm. Eng. 4(2014)32-41.

[9] H. Younes, M. Mao, S.M. Murshed, D.Lou, H. Hong, G.P. Peterson, Nanofluids: Key parameters to enhance thermal conductivity and its applications, Appl. Therm. Eng. 207(2022) 118-202.

[10] M.H. Fard, M.N. Esfahany, M.R. Talaie, Numerical study of convective heat transfer of nanofluids in a circular tube two-phase model versus single-phase model, Int. Commun. Heat Mass Transfer. 37(2010) 91-97.

[11] Z.Y. Ghale, M. Haghshenasfard, M.N. Esfahany, Investigation of nanofluids heat transfer in a ribbed microchannel heat sink using single-phase and multiphase CFD models, Int. Commun. Heat Mass Transfer. 68(2015) 122-129.

[12] J. Niu, C. Fu, W. Tan, Slip-flow and heat transfer of a non-Newtonian nanofluid in a microtube, PLoS One. 7 (5) (2012) e37274.

[13] R. Sadri, A.R. Mallah, M.Hosseini, G.Ahmadi, S.N. Kazi, A. Dabbagh, C.H. Yeong, R. Ahmad, N.A. Yaakup, CFD modeling of turbulent convection heat transfer of nanofluids containing green functionalized graphene nanoplatelets flowing in a horizontal tube: Comparison with experimental data, Journal of Molecular Liquids. 269(2018) 152-159.

[14] S. Kakaç, A. Pramuanjaroenkij, Review of convective heat transfer enhancement with nanofluids, International Journal of Heat and Mass Transfer. 52(2009) 3187-3196

[15] V. Bianco, F. Chiacchio, O. Manca, S. Nardini, Numerical investigation of nanofluids forced convection in circular tubes, Appl. Therm. Eng. 29(2009) 3632-3642.

[16] S.E.B. Maiga, S.J. Palm, C.T. Nguyen, G. Roy, N. Galanis, Heat transfer enhancement by using nanofluids in forced

convection flows, Int. J. Heat Fluid Flow. 4(2005) 530-546.

[17] H. Almohammadi, Sh. Nasiri Vatan, E. Esmaeilzadeh, A. Motezaker, A. Nokhosteen, Experimental investigation of convective heat transfer and pressure drop of Al_2O_3/Water nanofluid in Laminar flow regime inside a circular tube, International Journal of Mechanical and Mechatronics Engineering. 6(2012) 1750-1755.

[18] S.Z. Heris, T.H. Nassan, S.H. Noie, CuO/water nanofluid convective heat transfer through square duct under uniform heat flux, Int. J. Nanosci. Nanotechnol. 7(2011) 111-120.

[19] O. Benzeggouta, T. Boufendi, S. Touahri, Comparative study of fluid flow and heat transfer between usual fluids and nanofluids in a heated horizontal pipe, Journal of Thermal Science and Technology. 13(2018) 1-13.

[20] N. Purohit, V.A. Purohit, K. Purohit, Assessment of nanofluids for laminar convective heat transfer: A numerical study, Engineering Science and Technology, an International Journal. 19(2016) 574-586.

[21] S.Z. Heris, F. Oghazian, M. Khademi, E. saeedi, Simulation of convective heat transfer and pressure drop in laminar flow of Al_2O_3/water and Cuo/water nanofluids through square and triangular cross-sectional ducts, Journal of Renewable Energy and Environment. 2(2015) 6-18.

[22] K. Madani, R.B. Maad, A.A. Saad, Numerical investigation of cooling a ribbed microchannel using nanofluid, Journal of Thermal Engineering. 4(2018) 2408-2422.

[23] M.K.Moraveji, M. Darabi, S. M. H. Haddad, R. Davarnejad, Modeling of convective heat transfer of a nanofluid in the developing region of tube flow with computational fluid dynamics, Int. Commun. Heat Mass Transfer. 38(2011) 1291-1295.

[24] V.M. Krishna, Heat transfer enhancement by using ZnO-Water nanofluid in a concentric tube heat exchanger under forced convection conditions, International Journal of Innovations in Engineering and Technology. 7(2016) 177-184.

[25] P. Kanti, K.V. Sharma, Z. Said , V. Kesti, Entropy generation and friction factor analysis of fly ash nanofluids flowing in a horizontal tube: Experimental and numerical study, International journal of thermal sciences. 166 (2021)106972.

[26] P.K. Kanti, K.V. Sharma, A. A. Minea, V. Kesti, Experimental and computational determination of heat transfer, entropy generation and pressure drop under turbulent flow in a tube with fly ash-Cu hybrid nanofluid. International journal of thermal sciences. 167(2021) 107016.

[27] A.M.Hussein, R.A. Bakar, K. Kadirgama, K.V. Sharma, Heat transfer enhancement using nanofluids in an automotive cooling system, Int. Commun. Heat Mass Transfer. 53(2014)195-202

[28] A.M. Hussein, R.A. Bakar, K. Kadirgama, K. V. Sharma, Heat transfer augmentation of a car radiator using nanofluids, Heat Mass Transfer. 50(2014) 1553–1561.

[29] Y.R. Sekhara, K.V. Sharmab, R.T. Karupparaja, C. Chiranjeevia, Heat transfer enhancement with Al_2O_3 nanofluids and twisted tapes in a pipe for solar thermal applications, Procedia Engineering. 64(2013) 1474-1484.

[30] U. K. Ahmada, M. Hasreena, N. A. Yahaya, B. Rosnadiah, Comparative study of heat transfer and friction factor characteristics of Nanofluids in rectangular channel, Procedia Engineering. 170(2017) 541-546.

[31] K. S. Arjun, K. Rakesh, Heat transfer enhancement using alumina nanofluid in circular micro channel, Journal of Engineering Science and Technology. 12(2017) 265-279.

[32] M.A. Ahmeda, M.M. Yaseena, M.Z. Yusoff, Numerical study of convective heat transfer from tube bank in cross flow using nanofluid, Case Stud. Therm. Eng. 10(2017) 560-569.

[33] Mohammad Sikindar Baba, A.V.S.R. Rajub, M.B. Raoc, Heat transfer enhancement and pressure drop of Fe3O4–water nanofluid in a double tube counter flow heat exchanger with internal longitudinal fins, Case Stud. Therm. Eng .12(2018) 600-607.

[34] A. Abdollahi, H.A. Mohammed, S.M. Vanaki, R. N. Sharma, Numerical investigation of fluid flow and heat transfer of nanofluids in microchannel with longitudinal fins, Ain Shams Engineering Journal. 9(2018) 3411-3418.

[35] M.Gupta, N.Arora, R.Kumar, S.Kumar, N.Dilbaghi, A comprehensive review of experimental investigations of forced convective heat transfer characteristics for various nanofluids, International Journal of Mechanical and Materials Engineering. 9(2014) 1-21.

[36] U. Akdag, S. Akcay, D. Demiral, Heat transfer enhancement with nanofluids under laminar pulsating flow in a trapezoidal-corrugated channel, Progress in Computational Fluid Dynamics. 17(2017) 302-310.

[37] Y. Hu, Y. He, H. Gao, Z. Zhang Forced convective heat transfer characteristics of solar salt-based SiO2 nanofluids in solar energy applications, Appl. Therm. Eng. 155(2019) 650-659.

[38] M. Hejri, M. Hojjat, S.G. Etemad, Numerical simulation of nanofluids flow and heat transfer through isosceles triangular channels, Journal of Particle Science and Technology. 4(2018) 29-38.

[39] K. Khanafer, K. Vafai, M. Lightstone, Buoyancy-driven heat transfer enhancement in a two-dimensional enclosure utilizing nanofluids, Int. J. Heat Mass Transfer. 46 (2003) 3639-3653.

[40] H. C. Brinkman, The viscosity of concentrated suspensions and solution. J. Chem. Phys. 20(1952) 571-581.

[41] R. Mondragon, D. Sanchez, R. Cabello, R. Llopis, J.E. Julia, Flat plate solar collector performance using alumina nanofluids: Experimental characterization and efficiency tests, PLoS ON. 14(2)(2019) e0212260.

[42] J.C. Maxwell, A Treatise on Electricity and Magnetism, second ed. Oxford University Press, Cambridge. (1904) 435-441.

[43] A. Bouaffane, K. Talbi, Thermal study of fluid flow inside an annular pipe filled with porous media under local thermal non-equilibrium condition, Journal of Mechanical Engineering and Sciences. 13(2019) 4880-4897.

[44] A.M. Ali, M. Angelino, A. Rona, Numerical analysis on the thermal performance of microchannel heat sinks with Al_2O_3 nanofluid and various fins, Appl. Therm. Eng. 198(2021) 117458.

[45] M. Izadi, A. Behzadmehr, D.J. Vahida, Numerical study of developing laminar forced convection of a nanofluid in an Annulus, Int. J. Therm. Sci. 48(2009) 2119-2129.

[46] A. Aghanajafi, D. Toghraie, B. Mehmandoust, Numerical simulation of laminar forced convection of water-CuO nanofluid inside a triangular duct, Physica E. 85(2017)103–108,

[47] R. M. Cuenca, R. Mondragon, L. Hernandez, C. Segarra, J.C. Jarque, T. Hibiki, J.E. Julia, Forced-convective heat-transfer coefficient and pressure drop of water-based nanofluids in a horizontal pipe, Appl. Therm. Eng. 98(2016) 841-849.

[48] M. N. Ozisik, Heat transfer A Basic Approach, (1985) McGraw-Hill Book Company.

[49] S.V. Patankar, Numerical heat transfer and fluid flow, (1980). Hemisphere Publishing Corporation, Taylor and Francis Group, New York.

[50] H. Haithem, S. Touahri, T. Boufendi, Conjugate heat transfer in an annulus with heated longitudinal and transversal fins, International Journal of Thermofluid Science and Technology. 10(2)(2023) 1-14

[51] William S. Janna, Engineering heat transfer , 2nd edition (2000), United States of America.

[52] Yunus A. Cengel, Introduction to thermodynamics and heat transfer. (1997) McGraw-Hill companies, United State of America.

[53] M. J. H. Munshi, M. S. Islam, M. R. R. Khandaker, M. S. Hossain, Simulation of nanofluid flow in porous square-shaped enclosures, Journal of Scientific Research. 15 (2023) 383-399